Investigation of NO Reduction by H_2 on Pd Monolith with Transient and Isotopic Exchange Techniques

II. H_2/D_2 Exchange in the Reduction of NO

K. Rahkamaa-Tolonen,[*,1] T. Salmi,[*] D. Yu. Murzin,[*] L. Barreto Dillon,[*] U. Lassi,[†] and R. L. Keiski[†]

Laboratory of Industrial Chemistry, Process Chemistry Group, Faculty of Chemical Engineering, Åbo Akademi, FIN-20500 Turku-Åbo, Finland; and †Department of Process and Environmental Engineering, University of Oulu, FIN-90014 Oulu, Finland

The kinetics and mechanism of catalytic reduction of nitrogen oxide (NO) by hydrogen on an alumina-based palladium monolith were studied under atmospheric pressure at 155°C. Transient kinetic experiments, as well as isotopic exchange techniques, were applied in order to improve understanding of the reactions occurring on the surface of the noble metal catalyst. Nitrogen, nitrous oxide, ammonia, and water were detected as reaction products in the reduction of nitrogen oxide by hydrogen. The dissociation of NO on the catalyst surface is the crucial step affecting the overall reaction. Ammonia was formed by stepwise hydrogenation of adsorbed nitrogen atoms, which was confirmed by isotope transient techniques. Reaction pathways explaining the reduction of NO with hydrogen and deuterium were proposed. © 2002 Elsevier Science (USA)

Key Words: nitrogen oxides; hydrogen; deuterium; reduction; palladium; monolith; transient kinetics; isotopic exchange; TPD.

1. INTRODUCTION

Emissions from vehicles are suppressed by catalytic conversion, i.e., total oxidation of carbon monoxide and hydrocarbons and reduction of nitrogen oxides. In environmental catalysis, the main issue is to optimise catalytic converters to remove pollutants. Therefore, a detailed understanding of the kinetic processes is needed. The reaction mechanisms for the abatement of nitrogen oxides (NO_x) are of particular interest, since they are environmentally very unfriendly compounds. Most of the modern vehicles have after-treatment devices, typically monolithic catalytic converters, to transform pollutants in the exhaust gas to less harmful components. A principally straightforward way to remove NO would be self-decomposition. The noncatalytic reaction is retarded by the high activation energy ($E_a > 364$ kJ/mol) (1). Kinetically, the reaction rate can be enhanced via decreasing the activation energy with an effective catalyst. The main obstacle of the self-decomposition of NO and N_2O is, however, the strong oxygen adsorption on most

catalysts, which leads to the decay in active NO_x-adsorption sites and causes a rapid decline in the catalyst activity (2, 3). Therefore, selective catalytic reduction (SCR) has turned out to be a more successful way to remove NO. The current SCR technology uses NH_3; however, there are drawbacks with this process and the utilisation of other reductants, such as CH_4, CO, and H_2, is desirable (4). Hydrogen can act as a reductant of NO on noble metal catalysts, provided the concentration of O_2 is low in the exhaust gas (5). In the presence of excess of O_2, hydrogen is easily consumed in the simple combustion with O_2 (6, 7), but not in the reactions with nitrogen oxides. As a result of the thermal cracking reactions that take place in the flame, especially with incomplete combustion, hydrogen is formed and emitted, as are hydrocarbons that are different from the ones present in the fuel (8). It is, therefore, worth revealing the surface reaction mechanisms of NO_x reduction by H_2. One of the main practical applications of transient methods in catalytic kinetics has been undoubtedly the study of transient behaviour of three-way automotive catalysts. It is well-known that these catalysts normally operate under transient conditions (9, 10). Fundamental knowledge related to elementary reaction kinetics and mechanisms on single-metal components of three-way catalysts will also be indispensable in the design of improved converters. In the present work, the catalytic reduction of NO by H_2/D_2 was investigated with transient step-response experiments. Isotopic exchange experiments provide information on the behaviour of the reactants. Deuterium step changes were utilised also to trace the hydrogen reaction pathways during the water and ammonia formation. The adsorption and dissociation of NO was examined by temperature-programmed desorption (TPD).

2. EXPERIMENTAL

2.1. Catalysts

Pd-based metallic catalysts provided by Kemira Metalkat Oy (Finland) were used in this study. The catalyst sample

---

consisted of flat and corrugated metal foils coated with a support, mainly containing γ-Al$_2$O$_3$. Noble metals were impregnated on the support in an aqueous solution. The support material content of the alumina-supported Pd (3%) catalyst was 40 g/m^2 and the metal amount in the washcoat was 3 wt%. The BET surface area of the catalyst determined by nitrogen physisorption was 106 m^2/g. The pore volume of the catalyst was 0.32 cm^3/g and the mean pore diameter was 12 nm. The palladium particle size characterised by carbon monoxide chemisorption was about 12 nm. A detailed description of the 1% Pd on the alumina-supported catalyst can be found in the preceding part of the present work (11); the most pertinent details are given below. The support material content of the 1% Pd catalyst was 41 g/m^2. The BET surface area of the Pd catalyst was 112 m^2/g. The pore volume of the catalyst was 0.33 cm^3/g and the mean pore diameter was 12 nm. The palladium particle size was about 3.2 nm.

2.2. NO-TPD Experiments

NO-TPD (temperature-programmed desorption) measurements were carried out to obtain information on the surface adsorption states of the Pd-based catalysts supported on γ-alumina. Adsorption of NO on 1% Pd and 3% Pd catalysts was studied in order to determine the effect of the amount of palladium on the adsorption and desorption. Analogous experiments were carried out over the alumina support, too, mainly consisting of γ-alumina, to evaluate the effect of the support material on the surface adsorption states. The volume of the catalyst monolith was 1.4 cm^3. In the pretreatment stage, catalysts were evacuated for 2 h and then reduced under hydrogen flow for 10 min at 500°C. The catalysts were exposed to 5% NO/Ar at room temperature for 10 min. The gas flows were regulated with mass flow controllers (Bronkhorst). The NO-TPD measurements were carried out in a quartz chamber in vacuum at 30–800°C at a linear heating rate of 30°C/min. A split of a product gas flow was taken through a capillary into a quadrupole mass spectrometer (Carlo Erba Instruments Q.T.M.D.). The experimental setup for the NO-TPD measurements is presented in detail in our earlier publication (12).

2.3. Experimental Procedure of Step-Response Experiments

Reduction of NO with hydrogen was studied with transient step-response experiments. A single step of both reactants was performed under different concentration conditions (stoichiometric, excess of NO, and excess of H$_2$). Pretreatments with NO and H$_2$ were carried out to investigate their effect on the final concentration of products and on transient kinetics. Tracing the hydrogen pathway by D$_2$ contributes to the understanding of the role of hydrogen in the reduction of NO. Hydrogen was replaced by deuterium

after the steady state was attained during the NO + H$_2$ reaction. Calibration was carried out with gas mixtures containing known concentrations of the components before displaying the NO + H$_2$ data as mole fractions in tables and figures. For deuterium-containing products, the total signal for each m/z value divided by the signal of a carrier gas is shown in Figs. 6–8. The experimental procedure is described in detail in the previous part of the present article (11).

3. RESULTS AND DISCUSSION

3.1. Temperature-Programmed Desorption of NO

NO (at $m/z = 30$), N$_2$ (at $m/z = 28$), O$_2$ (at $m/z = 32$), and N$_2$O (at $m/z = 44$) were the main desorption products from these catalysts, whereas no formation of NO$_2$ (at $m/z = 46$) was detected. This is consistent with the results of Huang *et al.* (13) and Valden *et al.* (14), who have conducted NO-TPD experiments on the same type of catalyst surfaces. It is, however, difficult to draw conclusions between peak maxima and positions, due to the different pretreatment procedures and heating rates they used.

Figures 1a–1d show the comparative TPD curves for the individual desorption products from the alumina support, 1% Pd/alumina and 3% Pd/alumina catalysts, following adsorption of 5% NO/Ar at room temperature for 10 min. The adsorption of NO on catalysts occurred mainly molecularly, as indicated by the large amounts of NO desorbed and small amounts of N$_2$O and N$_2$ formation as a result of partial dissociation of NO during heating. Two prominent NO-TPD peaks for the support were observed, at around 310 and 480°C (Fig. 1a). The lower temperature state of NO was dominant and had a higher adsorption capacity. For the 1% Pd catalyst, three adsorption states were observed, at temperatures around 250, 310, and 440°C. The lowest temperature NO state was caused by NO–Pd interaction, because it was not observed in the case of the support material. The middle state was observed as the shoulder in a TPD spectrum consisting mainly of the interaction between NO and support material. The highest temperature state was due to NO support as well as NO–Pd interaction. It can be concluded that the interaction between NO and alumina support was significant, which has also been observed by other researchers (14, 15). Thus, the support itself is active and a strong adsorption of NO onto the support was observed.

In the literature, there has been a lot of discussion on the number and the origin of NO-TPD peaks on alumina-based catalyst surfaces. Huang *et al.* (13) observed three peaks, at 100, 410, and 530°C after NO adsorption; in contrast, Kijlstra *et al.* (16) observed only two peaks, at 180 and 375°C. The differences in temperature maxima might be due to different heating rates. Peak maxima are shifted to higher temperatures when heating rate is increased (15).
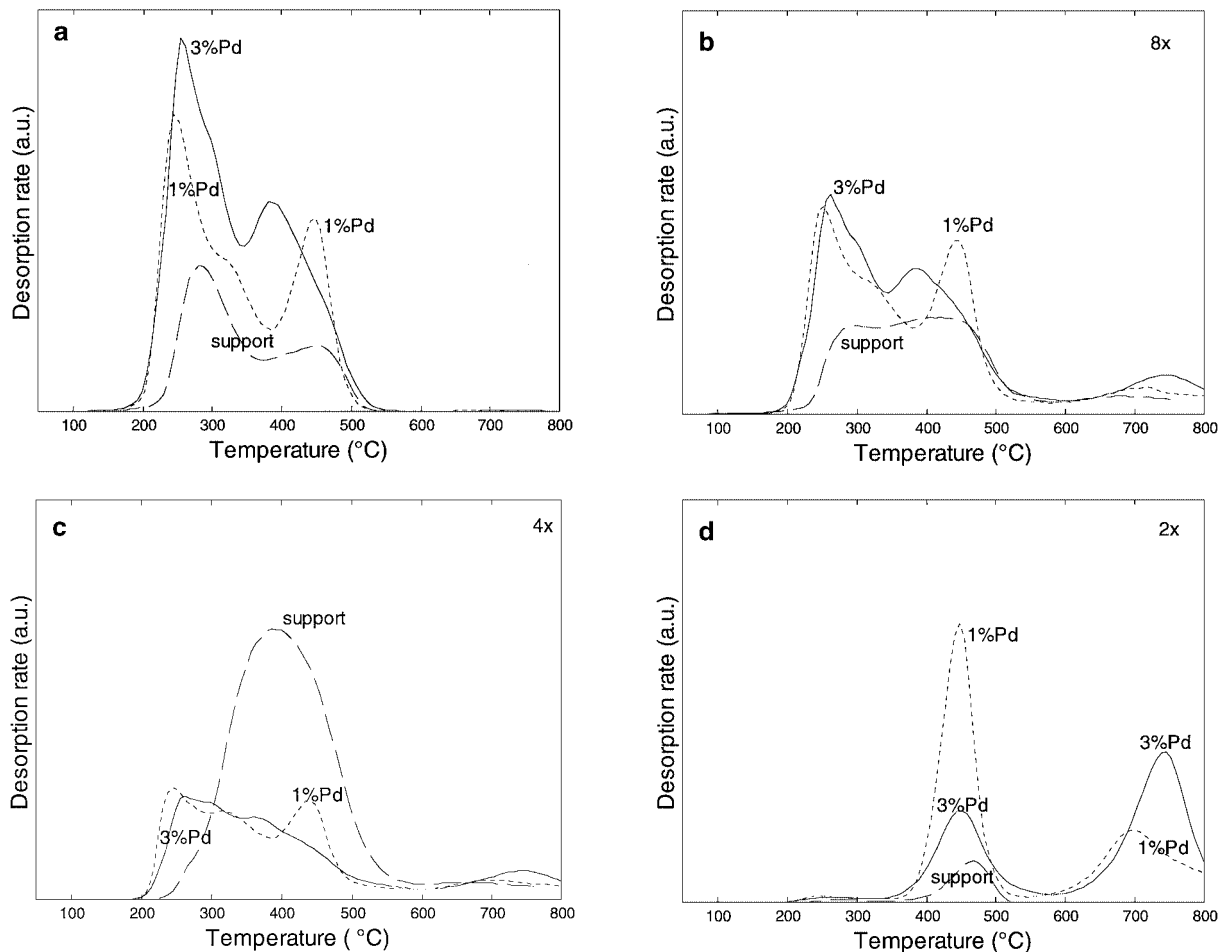
FIG. 1. TPD spectra of (a) NO, (b) N_2, (c) N_2O, and (d) O_2 for the alumina support, 1% Pd/alumina and 3% Pd/alumina, following adsorption of 5% NO at room temperature (25°C) for 10 min. Heating rate: 30°C/min.

The origin of the lower temperature adsorption state of NO is not well understood. The highest temperature NO-TPD peak was accompanied by oxygen desorption, and this corresponds to the decomposition of nitrate and nitrite species (14, 16). This explanation is supported also by our experiments where oxygen desorption occurred in the same temperature range as the highest temperature NO adsorption state observed, around 440°C (Figs. 1a and 1d).

N_2, N_2O, and O_2 were formed over the alumina support, 1% Pd/alumina and 3% Pd/alumina catalysts, as can be seen from Figs. 1b–1d. Especially, the formation of N_2O on the support was remarkable. This might be due to Zr, La, and Ce oxides present in the support. In addition to TPD, adsorption of NO was studied by a step-response experiment from Ar to a 1% NO/Ar mixture at 155°C with the Pd catalyst and the support. After the switch (400 s) mole fractions of formed N_2O and N_2 were 1.0×10^{-4} on the Pd catalyst and the mole fraction of formed N_2O was 4.0×10^{-5} on the support alone. The transient response of N_2O was higher than that of N_2 in the beginning of the experiment

with the Pd catalyst. On the support nitrogen was formed only during the first 15 s after the switch. In addition to TPD, these step-response experiments also confirmed the N_2O formation on the support. The formation of N_2 and N_2O was observed in small amounts in the same temperature range where NO desorption occurred, with maxima at around 250 and 440°C over 1% Pd/alumina. We conclude that palladium metal particles are mostly responsible for the decomposition of NO, because the formation of N_2O was smaller and the formation of N_2 was higher in the case of 1% and 3% Pd catalysts than in the case of support (Figs. 1b and 1c). The TPD results of NO from the alumina-supported Pd catalysts in this study are consistent with those of Valden *et al.* (14) and Ciuparu *et al.* (17), who also demonstrated that palladium particles have a central role in the decomposition of NO.

According to Fig. 1d, oxygen desorption occurred as a single sharp peak around 470°C for the support. In the case of 1% Pd/alumina and 3% Pd/alumina catalysts, oxygen desorbed in two states, having also a higher temperature state
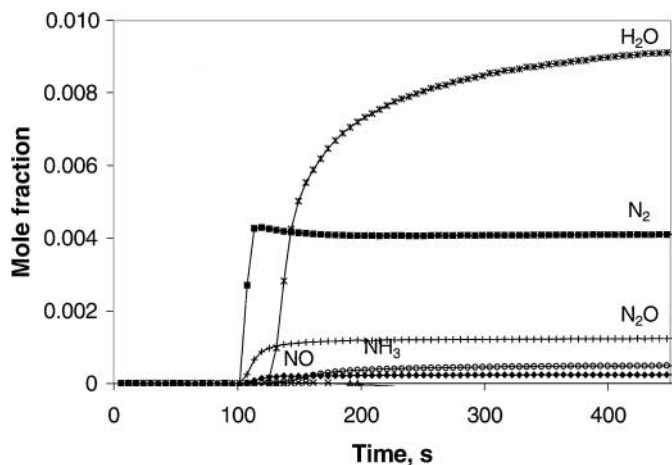
FIG. 2. Ar → (1% NO + 1% H$_2$)/Ar step-response experiment on the Pd catalyst at 155°C.

at around 750°C. The origin of this state is not fully known, but it is somehow related to the oxidation states of palladium because it was not observed in the case of support. Palladium oxide supported on alumina is found to decompose to metallic palladium at around 700–800°C, depending on the oxygen partial pressure (18). It can also be observed that the support was almost inactive in oxygen formation.

3.2. Reduction of NO with H$_2$

From Figs. 2–7 it can be seen that NO reduction with H$_2$ generated H$_2$O and N$_2$ as the main products and N$_2$O and NH$_3$ as the by-products. The responses of the reduction of NO + H$_2$ with 1% of each reactant in the reacting mixture are shown in Fig. 2. During the first 350 s after the step change from Ar to the reaction mixture, the temperature increased from 155 to 180°C. A slight maximum in the nitrogen response was detected at the beginning of the NO + H$_2$ step. Water and ammonia started to liberate once N$_2$, N$_2$O, and NO had almost reached the steady state.

Figure 3 shows the responses of reduction of NO with H$_2$ after a pretreatment with NO. Figure 3a presents a step response from Ar to a 1% NO/Ar mixture with the reduced Pd catalyst at 155°C. Minimal amounts of N$_2$O and N$_2$ were formed. The transient response of N$_2$O was higher than that of N$_2$ in the beginning of the experiment. After introducing H$_2$ to the reactor, the response of N$_2$O appeared first (Fig. 3b). Nitrogen-containing species reached their steady states faster than water.

Figure 4 shows the transient responses of the reduction of NO with H$_2$ with a pretreatment of hydrogen. Once H$_2$ entered the monolith, the steady state was reached almost immediately, with minor formation of water. Hydrogen molecules easily adsorb and dissociate on palladium, due to the low activation energy for adsorption (19). The surface of the catalyst was then covered by atomic hydro-
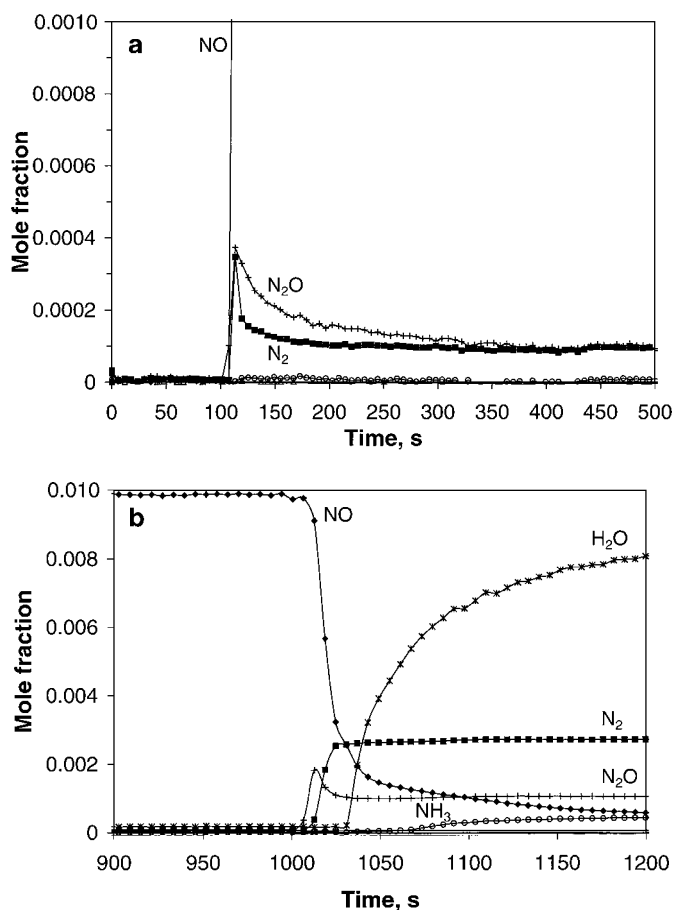

FIG. 3. Ar → 1% NO/Ar → (1% NO + 1% H$_2$)/Ar step-response experiment on the Pd catalyst at 155°C: (a) Ar → 1% NO/Ar step; (b) 1% NO/Ar → (1% NO + 1% H$_2$)/Ar step.

gen, which reacts with the OH groups present in the oxide catalyst, releasing a small amount of water, as can be seen from Fig. 4. The isotopic exchange experiment of H$_2$ and D$_2$ on the support material provided the supporting
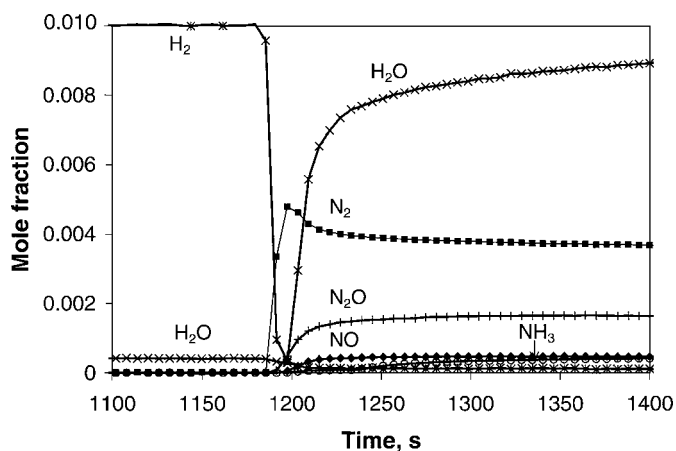

FIG. 4. 1% H$_2$/Ar → (1% NO + 1% H$_2$)/Ar step-response experiment on the Pd catalyst at 155°C.

evidence for water formation (11). During this experiment a small amount of H_2O was formed also on the modified alumina support. When NO was introduced into the reactor, a N_2 response was immediately observed but it decreased quickly. The second product formed was N_2O, which indicated the abundance of NO^* and N^* species on the surface. The formation of water started again after the N_2 and N_2O responses had almost reached their steady states. The NH_3 response was rather slow.

In the case of no catalyst pretreatment and H_2 pretreatment, a maximum in the response of N_2 was detected when NO was introduced into the reactor. The more intensive one was obtained after the H_2 pretreatment. The N_2 response decreased quickly, possibly because of the decrease in activity of the catalyst due to the oxygen, water, and hydroxyl accumulation on the surface (20). The nitrogen response was the fastest, which indicated rapid dissociation of NO on the metallic surface. The explanation might be the availability of the reductant.

The response of N_2O differed considerably in the NO pretreatment experiment compared to the experiments without and with H_2 pretreatment during the transient period. In the case of NO pretreatment, a maximum for the N_2O response was detected as H_2 was introduced into the monolith. In the other two cases, the N_2O response reached the steady state rapidly without showing any maximum. For the H_2 pretreatment experiment, a small decline was detected in the middle of the NO + H_2 step, then the steady state was quickly attained.

The NH_3 responses in all three cases reached the steady state at the same time. The shape of the responses and the mole fraction of NH_3 at steady state were similar. The responses of H_2O did not differ significantly; they showed the similar transient responses, reaching the steady state almost at the same time.

The conversion of NO and the relative product distribution with respect to N and H atoms at steady state in the NO and H_2 experiments (1% NO/Ar and 1% H_2/Ar pretreatment as well as without any pretreatment) are shown in the Table 1. In these three cases, high conversions, which were in practice equal, were obtained. Selectivity towards N_2, N_2O, and NH_3 at steady state did not vary significantly.

NO showed the highest relative product distribution with respect to N atoms towards N_2, as revealed by Table 1. It was slightly higher for the experiments without any pretreatment and values were close for pretreatment experiments. N_2O was the second most abundant nitrogen component into which NO converts in all three cases. The mole fractions of N_2O at the steady state were practically equal for all cases. The selectivity of NO with respect to ammonia was small in all three cases.

The relative product distribution with respect to H atoms during the steady state is also presented in Table 1. Water was clearly the most abundant product in the three cases. Preferentially H_2O was formed from hydrogen atoms. The ammonia formation was rather minor, reaching 5% in all cases.

The relative amount of N, NO, and H adsorbed on the surface are the key factors determining the selectivity. Therefore, during the transient period of the experiments there was a small variation in selectivity towards N_2, N_2O, and NH_3. However, it can be concluded that transient periods of the experiments were fractionally different due to different surface coverages in the beginning of the experiments, but in steady state catalysts reached similar states.

Once NO and H_2 were introduced into the reactor in the case of no catalyst pretreatment, all the active sites of the catalyst were free and started to be initially covered by NO^* and H_2^*. At this point there were still many vacant sites, which enhanced the dissociation of NO^* into N^* and O^*, as explained by Hirano et al. (21). High coverage of N^* on the surface promoted the formation of diatomic nitrogen, which was detected to be the primary reaction product of NO. N_2O was also produced due to the presence of NO^* and N^*:

$$NO^* + N^* \rightarrow N_2O + 2^*. \qquad [1]$$
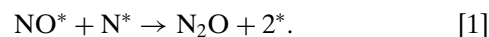
Therefore, in the case of no catalyst pretreatment the probability of forming N_2 was higher than in the case of NO pretreatment, where NO pretreatment has an oxidising effect. It is known that NO dissociation is favoured on metallic Pd sites. In the case of pretreatment by NO, N_2O was the first product seen and there was a maximum in the N_2O response after introduction of the reaction mixture because

TABLE 1

Conversion of NO and Relative Product Distribution with Respect to N Atoms from NO and H Atoms from H_2 during the Steady State (1% NO + 1% H_2 in Ar) over the Alumina-Based Pd Catalyst

Experiment	NO conversion	Relative product distribution with respect to N atoms			Relative product distribution with respect to H atoms	
		N_2	N_2O	NH_3	H_2O	NH_3
Without pretreatment	0.98	0.69	0.22	0.09	0.95	0.05
Pretreatment with NO	0.96	0.64	0.24	0.12	0.95	0.05
Pretreatment with H_2	0.97	0.66	0.25	0.09	0.95	0.05

NO was preadsorbed on the surface and the dissociation of only one NO molecule is needed for the formation of N$_2$O (Fig. 3b). The changes in relative amounts of NO* and N* coverages on the catalyst surface explained the maximum in the response of N$_2$O. NO adsorption as well as oxidation of metallic clusters blocked active sites for hydrogen dissociation and thus enhanced the incomplete reduction to N$_2$O. Gas-phase oxygen was not observed during the NO pretreatment experiment. This could be explained by the strong adsorption of oxygen atoms on the metal surface, which was confirmed by the NO-TPD experiments (Fig. 1d).

This fact explains the peaks in N$_2$O and N$_2$ responses detected at the beginning of the NO step, when still some active sites of the catalyst are vacant and allow the dissociation of NO* to N* and O* (Fig. 3a). The N$_2$ signal was slightly lower than the N$_2$O signal in the beginning of the step reponse. Once NO enters the monolith, it is adsorbed on the metal surface. NO oxidises the surface of the catalyst. Previous studies have demonstrated that NO dissociation does not proceed on surfaces fully covered with NO at low temperatures (18). It is well established now that the dissociation of NO requires the existence of vacant sites in the neighbourhood of the adsorbed molecule. For the selectivity of NO to N$_2$ or N$_2$O, the availability of a vacant site adjacent to NO* and N* plays a crucial role. In this case, nitrogen was formed, as NO started to cover the surface of the catalyst, but there existed still vacant sites for the dissociation of NO. However, once the active sites were covered by NO* and O*, the formation of N$_2$O became higher and it then decreased with the coverage of NO, indicating that Pd was not an effective catalyst for the self-decomposition of NO. Our NO-TPD result showed that oxygen did not desorb before 380°C. Therefore, in the absence of any reducing agent the active sites were blocked by oxygen at temperatures below 380°C.

In the absence of H$_2$ only very little N$_2$ and N$_2$O were formed, as can be seen from Fig. 3a. Therefore, hydrogen is needed to react with O*, keeping the metal atoms available for reactions. Arena *et al.* (22) stated that hydrogen quickly reduces the nitrogen oxides species present over the noble metal, thus cleaning the surface of the catalyst. The catalyst became covered by H*, which reacted with O* to form O–H* and further H$_2$O*. A small amount of water was also formed through a reaction of spillover H and OH (11). Once the cleaning of the surface was completed, new sites were accessible for NO to adsorb and dissociate, forming N$_2$, for which a prominent signal was detected. Dissociation of NO is also needed for the formation of N$_2$O and NH$_3$.

The delay of H$_2$O and NH$_3$ responses in reaching the steady state is most probably due to the consecutive formation mechanism of water and ammonia as well as to the adsorption of water and ammonia on the support, which is confirmed by the adsorption–desorption experiments (11).

These experiments implied also that the desorption of H$_2$O is a slow step. According to Hirano *et al.* (21) NH* was easily formed, but then it was only slowly further hydrogenated, which might also be one reason for the slow response of NH$_3$. According to the study of the NO–H$_2$ reaction on Pd (111), hydrogen was adsorbed dissociatively on this surface, penetrating into the subsurface at very low temperature, already at −183°C (23). It has been found that in the formation of water the reaction between O* and H$_{bulk}$ is preferred over the reaction of adsorbed oxygen with H* adsorbed on the surface. Therefore, the formation rate of H$_2$O was dominated by the transport of atomic hydrogen between the bulk and the surface. Formation of NH$_3$ might follow an analogous pathway. In the current study, this behaviour is supposed to be the least likely explanation for the delay of responses of hydrogen-containing species.

Step-response experiments from Ar to 1% NO/Ar and (1% NO + 1% H$_2$)/Ar mixtures at 155°C were carried out on the support to clarify the role of the support material. The consumed amount of NO was 0.184 mmol/g washcoat during the NO adsorption experiment. A minor amount of N$_2$O was formed on the support. A very small amount of nitrogen was formed only during 15 s at the beginning of the switch. The result indicated that the adsorption of NO and formation of N$_2$O happened on the support material to some extent. During the (1% NO + 1% H$_2$)/Ar experiment, a small amount of H$_2$O was formed on the modified alumina support. Minor amounts of N$_2$O and NH$_3$ were also formed. The N$_2$ response was visible for 15 s at the beginning of the experiment. This implied that only a small amount of NO dissociated on the support. After the switch from H$_2$ to D$_2$, very small amounts of HD and HDO were formed. Previous H$_2$/D$_2$ experiments (11) indicated that H$_2$ and D$_2$ dissociated and the exchange reaction with hydrogen and deuterium happened on the support material. The experiments also implied that OH groups from alumina can take part to some extent in the water formation. In addition, adsorption experiments (11) on the support material have shown that large amounts of NH$_3$ and H$_2$O are adsorbed on the support.

According to Hecker and Bell (24) and Burch and Watling (25) the fast enhancement of the rate of NO decomposition by H$_2$ is probably due to H-assisted NO decomposition. NO decomposition occurs by the following reaction:

$$NO^* + H^* \rightarrow N^* + OH^*. \qquad [2]$$
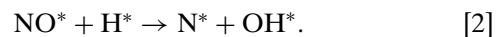
However, the most recent evaluation of single-crystal data concludes that both reactions can be adequately explained by an initial direct dissociation of NO followed by removal of the fragments by adsorbed reductant (26). Thus, based on the transient responses, the following mechanism for the abatement of NO over the Pd monolith is proposed. The nitrogen-containing reaction products N$_2$, NH$_3$, and N$_2$O
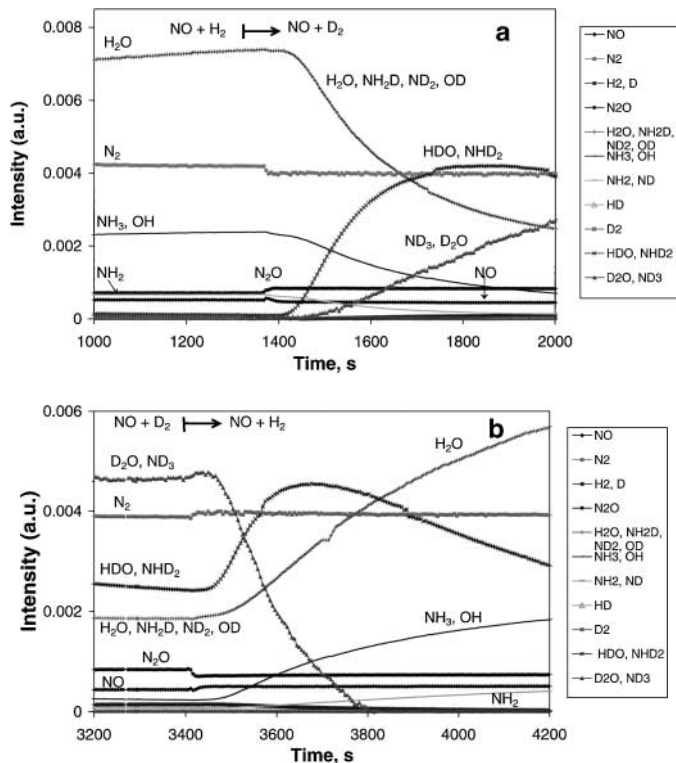
FIG. 5. Ar → (1% NO + 1% H_2)/Ar → (1% NO + 1% D_2)/Ar → (1% NO + 1% H_2)/Ar → Ar step-response experiment on the Pd catalyst at 155°C: (a) (1% NO + 1% H_2)/Ar → (1% NO + 1% D_2)/Ar step; (b) (1% NO + 1% D_2)/Ar → (1% NO + 1% H_2)/Ar step.

are formed via dissociation of NO:

$$NO + * \rightleftharpoons NO^*, \qquad [3]$$
$$NO^* + * \rightleftharpoons N^* + O^*. \qquad [4]$$

N_2 is formed by combination of two adatoms of nitrogen:

$$2N^* \rightleftharpoons N_2 + 2^*. \qquad [5]$$

At lower temperatures N_2 may also be formed via

$$NO^* + N^* \rightarrow N_2 + O^* + *. \qquad [6]$$

N_2O is formed by combination of adsorbed NO and nitrogen (Eq. [1]).

From Fig. 3b it can be seen that the abundance of NO^* promotes reaction [1] at the expense of reactions [5] and [6]. In contrast H^* contributes to reaction [5] (Fig. 4).

The most probable mechanism for ammonia formation is stepwise hydrogenation of adsorbed nitrogen atoms:

$$N^* \underset{-H^*}{\overset{+H^*}{\rightleftharpoons}} NH^* \underset{-H^*}{\overset{+H^*}{\rightleftharpoons}} NH_2^* \underset{-H^*}{\overset{+H^*}{\rightleftharpoons}} NH_3^*. \qquad [7]$$
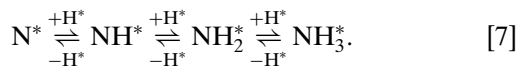
The surface oxygen reacts with dissociatively adsorbed hydrogen, forming surface hydroxyls, which are converted to

water:

$$O^* \underset{-H^*}{\overset{+H^*}{\rightleftharpoons}} OH^* \underset{-H^*}{\overset{+H^*}{\rightleftharpoons}} H_2O^*. \qquad [8]$$
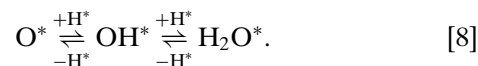
The isotopic transient experiments (Figs. 5–7) confirmed that ammonia and water were formed by stepwise hydrogenation, as is demonsrated in the following section.

3.3. Reduction of NO with H_2/D_2

Figures 5–7 show the transient states of the reduction of NO with hydrogen after an isotopic exchange with deuterium. Figure 5 shows the responses of the experiment carried out using equal amounts of reactants 1% NO + 1% H_2/D_2. The following two figures correspond to the results of experiments performed with different amounts of reactants, in which 2% NO + 1% H_2/D_2 (Fig. 6) and 1% NO + 2% H_2/D_2 (Fig. 7) have been used.

The switch from H_2 to D_2 is presented in the graphs shown in Figs. 5a, 6a, and 7a and the switch from D_2 to H_2 in the graphs shown in Figs. 5b, 6b, and 7b for the three different experiments carried out. During NO + H_2 step, the formation of water, nitrogen, ammonia, and nitrous oxide were detected, as discussed earlier. H_2O was the product
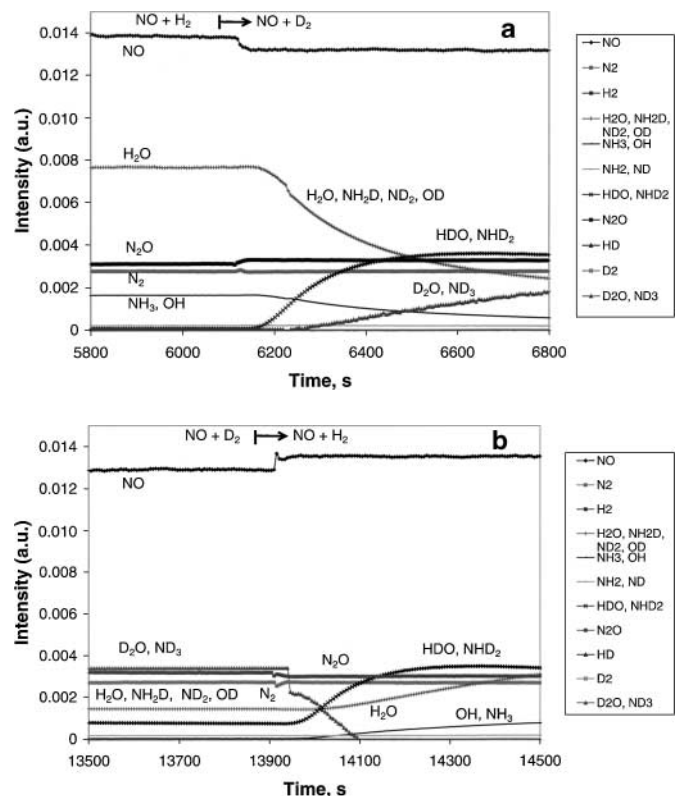

FIG. 6. Ar → (2% NO + 1% H_2)/Ar → (2% NO + 1% D_2)/Ar → (2% NO + 1% H_2)/Ar → Ar step-response experiment on the Pd catalyst at 155°C: (a) (2% NO + 1% H_2)/Ar → (2% NO + 1% D_2)/Ar step; (b) (2% NO + 1% D_2)/Ar → (2% NO + 1% H_2)/Ar step.
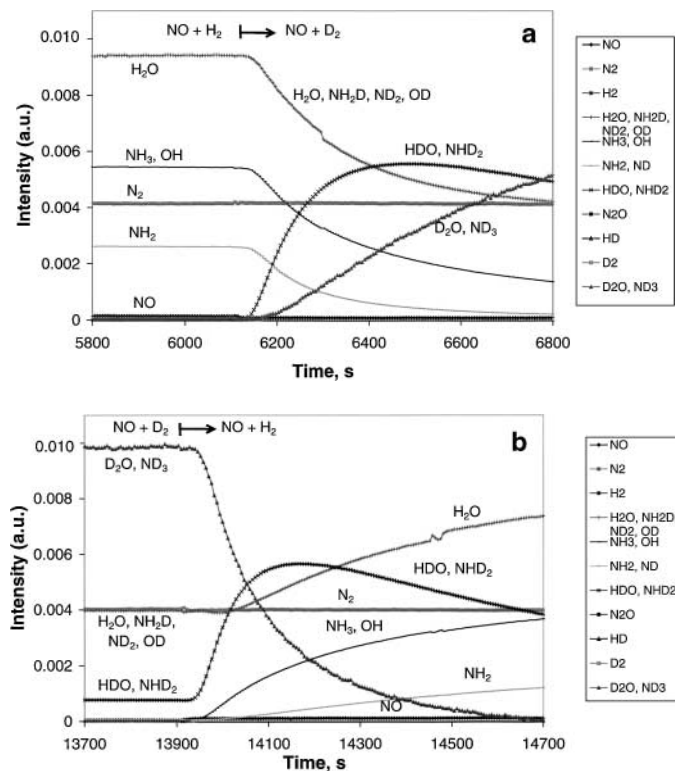
FIG. 7. Ar $\rightarrow$ (1% NO + 2% H$_2$)/Ar $\rightarrow$ (1% NO + 2% D$_2$)/Ar $\rightarrow$ (1% NO + 2% H$_2$)/Ar $\rightarrow$ Ar step responses on the Pd catalyst at 155°C: (a) (1% NO + 2% H$_2$)/Ar $\rightarrow$ (1% NO + 2% D$_2$)/Ar step; (b) (1% NO + 2% D$_2$)/Ar $\rightarrow$ (1% NO + 2% H$_2$)/Ar step.

mainly formed, having the highest value in steady state in the presence of excess H$_2$ (Fig. 7).

NH$_3$ formation was also detected in the three experiments, having the highest value in steady state when hydrogen was the excess reactant (Fig. 7), which corresponds with our earlier results (20). The signal of $m/z = 16$ (NH$_2$) was used to follow the formation of NH$_3$. This preference of forming NH$_3$ and H$_2$O when there was excess hydrogen deals with the availability of hydrogen atoms. The excess of hydrogen atoms allowed formation of hydrogen-containing species instead of N$_2$ or N$_2$O, even when the responses of these two last compounds were faster. In the excess of NO (Fig. 6) the amount of ammonia was much smaller than with stoichiometric and H$_2$-rich gas mixtures. This was caused by the lack of H* atoms to react with N*, which instead had many other N* and NO* in its surroundings to produce N$_2$ and N$_2$O.

Of the nitrogen-containing reaction products N$_2$ has the highest amount, with stoichiometric and H$_2$-rich gas mixtures. The amount of N$_2$O formed was higher than N$_2$ in excess NO (Fig. 6). This may be caused by the inhibition effect of adsorbed oxygen. Once the molecules of NO adsorbed on the surface they dissociated to form N* and O*. Since there was an excess of NO and probably few vacant sites on which NO* could dissociate, N* atoms had more NO*

molecules in their neighbourhood to react with and to form a higher amount of N$_2$O. Nitrous oxide, on the other hand, was not formed when an excess of hydrogen was present (Fig. 7). As can be seen in the figure, nitric oxide response was not clearly noticeable either, which indicated that the total dissociation of NO on the surface prevents the reaction of N* with chemisorbed NO*.

In addition to N$_2$, N$_2$O, and NH$_3$, the deuterium-containing reaction products HDO, D$_2$O, NH$_2$D, NHD$_2$, and ND$_3$ were observed. Formation of HD was not observed because D* reacts much faster with OH* or NH$_2^*$ than with H*, as discussed in the preceding part of the present work (11). Formation of products with $m/z = 20$, i.e., D$_2$O and ND$_3$, was detected to be the highest in all cases. Argon, which was used as a carrier gas, has a fragment of $m/z = 20$. The response of $m/z = 20$ is mainly attributed to deuterated water (D$_2$O), based on the fact that this compound behaves the same as H$_2$O. Therefore, its signal was similar to the response of water obtained in the NO + H$_2$ steps. Following the same behaviour as H$_2$O and NH$_3$, the amount of produced D$_2$O and ND$_3$ was highest in excess hydrogen (Fig. 7). Assuming that the ND$_3$ response followed more or less the same path as that of ammonia, it was possible then to relate part of the $m/z = 20$ response to ND$_3$ and thus recognise the behaviour of H$_2$O.

A peak in the response of $m/z = 17$ (HDO and NHD$_2$) was observed in the three experiments when the isotopic step change was performed (H$_2 \rightarrow$ D$_2$ and D$_2 \rightarrow$ H$_2$). These signals belonged mainly to HDO. The rest of this signal belonged to NHD$_2$. During the switch from H$_2$ to D$_2$, HDO response declined at the same time the D$_2$O response increased. This indicates that the formation of D$_2$O is via isotopic exchange of HDO* and D*, as was proposed in part I (11). The maximum in HDO and NHD$_2$ response during the isotopic step change from deuterium to hydrogen (Figs. 5b, 6b, and 7b) can be due to the reaction between the spillover deuterium on the support and the OH* as well as OH groups in the support. A small amount of it can be assigned to the NHD$_2$ formed via reaction between spill-over deuterium and NH*. The responses also showed that ND$_3$ is formed via stepwise deuteration. At the same time, the isotopic exchange in ammonia can take place, as was demonstrated in part I (11). It is difficult to estimate the relative importance of these two pathways due to the overlapping mass numbers.
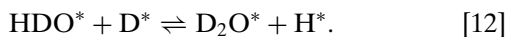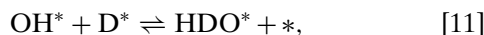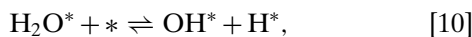
Based on the transient results, the mechanism for NO reduction with hydrogen and deuterium is proposed. Formation of N$_2$, N$_2$O, NH$_3$, and H$_2$O follows the mechanisms already mentioned above (Eqs. [1]–[8]).

Deuterium adsorbes dissociatively;
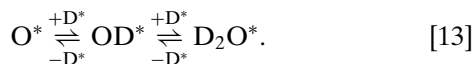
$$D_2 + 2^* \rightleftharpoons 2D^*. \qquad [9]$$

Formation of deuterated water can follow two different pathways. The first of them corresponds to the reaction of

dissociated water with deuterium:
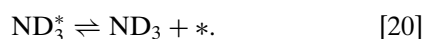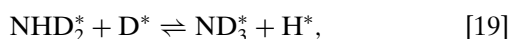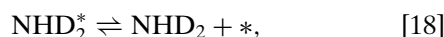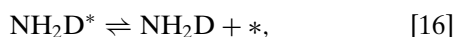
$$H_2O^* + * \rightleftharpoons OH^* + H^*, \qquad [10]$$

$$OH^* + D^* \rightleftharpoons HDO^* + *, \qquad [11]$$

$$HDO^* + D^* \rightleftharpoons D_2O^* + H^*. \qquad [12]$$

The second route is the stepwise one starting from atomically adsorbed oxygen:

$$O^* \underset{-D^*}{\overset{+D^*}{\rightleftharpoons}} OD^* \underset{-D^*}{\overset{+D^*}{\rightleftharpoons}} D_2O^*. \qquad [13]$$

Formation of ND_3 is also thought to follow two routes. In one hand, it can follow the H–D isotopic exchange in ammonia when there is some NH_3^* or NH_2^* available (as shown by separate experiments in part I):

$$NH_3^* + * \rightleftharpoons NH_2^* + H^*, \qquad [14]$$

$$NH_2^* + D^* \rightleftharpoons NH_2D^* + *, \qquad [15]$$

$$NH_2D^* \rightleftharpoons NH_2D + *, \qquad [16]$$

$$NH_2D^* + D^* \rightleftharpoons NHD_2^* + H^*, \qquad [17]$$

$$NHD_2^* \rightleftharpoons NHD_2 + *, \qquad [18]$$

$$NHD_2^* + D^* \rightleftharpoons ND_3^* + H^*, \qquad [19]$$

$$ND_3^* \rightleftharpoons ND_3 + *. \qquad [20]$$
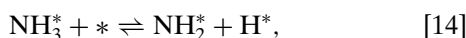
Another probable route is stepwise deuteration of adsorbed nitrogen:

$$N^* \underset{-D^*}{\overset{+D^*}{\rightleftharpoons}} ND^* \underset{-D^*}{\overset{+D^*}{\rightleftharpoons}} ND_2^* \underset{-D^*}{\overset{+D^*}{\rightleftharpoons}} ND_3^*. \qquad [21]$$
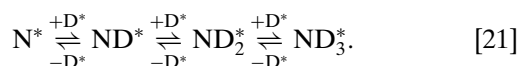
Further kinetic studies are needed to quantify the relative importance of these different routes.

4. CONCLUSIONS

The reduction of NO with H_2 and D_2 was studied with transient experiments on the Pd monolith. The experiments showed the complexity of the deuterated product formation in the deuteration step and provided a possible means of discriminating between different reaction mechanisms. Nitrogen, nitrous oxide, ammonia, and water were detected as reaction products in NO reduction by hydrogen. The dissociation of NO on the catalyst surface is the crucial step, dominating the overall reaction behaviour. Ammonia formation was favoured in excess H_2. Under NO-rich conditions the formation of N_2O was essentially higher than under H_2-rich or stoichiometric conditions. Ammonia and water were formed by stepwise hydrogenation of adsorbed nitrogen and oxygen atoms, respectively, which was confirmed by isotopic transient experiments.

REFERENCES

1. Glick, H. S., Klien, J. J., and Squire, W., *Chem. Phys.* **27**, 850 (1957).
2. Iwamoto, M., and Hamada, H., *Catal. Today* **10,** 57 (1991).
3. Iwamoto, M., and Yahiro, H., *Catal. Today* **22**, 5 (1994).
4. Armor, J. N., *Appl. Catal. B* **1**, 221 (1992).
5. Li, Y., and Armor, J. N., *J. Catal.* **150**, 376 (1994).
6. Iwamoto, M., and Takeda, H., *Catal. Today* **27**, 71 (1996).
7. Burch, R., Millington, P. J., and Walker, A. P., *Appl. Catal. B* **4**, 64 (1994).
8. Lox, E. S. J., and Engler, B. H., *in* "Handbook of Heterogeneous Catalysis" (G. Ertl, H. Knözinger, and J. Weitkamp, Eds.), Vol. 4, p. 1559. VCH, Weinheim, 1997.
9. Shelef, M., and Graham, G. W., *Catal. Rev.–Sci. Eng.* **36**, 433 (1994).
10. Taylor, K. C., *Catal. Rev.–Sci. Eng.* **35**, 457 (1993).
11. Rahkamaa-Tolonen, K., Salmi, T., Murzin, D. Yu., Barreto-Dillon, L., Karhu, H., Keiski, R. L., and Väyrynen, J., *J. Catal.*, in press.
12. Rahkamaa, K., Pulkkinen, U., Wärnå, J., Zhou, Y., Salmi, T., and Keiski, R. L., *in* "Proceedings of the 14th International Congress of Chemical and Process Engineering, Praha, August 2000," Czech Society of Chemical Engineering, Czech Republic, 2000.
13. Huang, S.-J., Walters, A. B., and Vannice, M. A., *Appl. Catal. B* **26**, 101 (2000).
14. Valden, M., Keiski, R. L., Xiang, N., Pere, J., Aaltonen, J., Pessa, M., Maunula, T., Savimäki, A., Lahti, A., and Härkönen, M., *J. Catal.* **161**, 614 (1996).
15. Falconer, J. L., and Schwarz, J. A., *Catal. Rev.–Sci. Eng.* **25**, 141 (1983).
16. Kijlstra, W. S., Brands, D. S., Poels, E. K., and Bliek, A., *J. Catal.* **171**, 208 (1997).
17. Ciuparu, D., Bensalem, A., and Pfefferle, L., *Appl. Catal. B* **26**, 241 (2000).
18. Farrauto, R. J., Hobson, M. C., Kennelly, T., and Waterman, E. M., *Appl. Catal. A* **81**, 227 (1992).
19. Miyazaki, E., *J. Catal.* **65**, 84 (1980).
20. Rahkamaa, K., Salmi, T., Keiski, R. L., Wärnå, J., and Zhou, Y., *Chem. Eng. Sci.* **56**, 1395 (2001).
21. Hirano, H., Yamada, T., Tanaka, K. I., Sierra, J., Cobden, P., and Nieuwenhuys, B. E., *Surf. Sci.* **262**, 97 (1992).
22. Arena, G. E., Bianchini, A., Centi, G., Vazzana, F., and Vitali, P., *Stud. Surf. Sci. Catal.* **122**, 109 (1999).
23. De Wolf, C. A., and Nieuwenhuys, B. E., *Surf. Sci.* **469**, 196 (2000).
24. Hecker, W. C., and Bell, A. T., *J. Catal.* **92**, 247 (1985).
25. Burch, R., and Watling, T. C., *Catal. Lett.* **37**, 51 (1996).
26. Nieuwenhuys, B. E., *Adv. Catal.* **44**, 249 (2000).